HHS Public Access

Author manuscript

Ther Deliv. Author manuscript; available in PMC 2017 August 23.

Published in final edited form as:

Ther Deliv. 2010 August ; 1(2): 307–322.

Advances in image-guided intratumoral drug delivery techniques

Luis Solorio[1], **Ravi B Patel**[1], **Hanping Wu**[1], **Tianyi Krupka**[1], and **Agata A Exner**[1,†]

[1]Case Western Reserve University, 11100 Euclid Ave., Cleveland, OH, 44106, USA

Abstract

Image-guided drug delivery provides a means for treating a variety of diseases with minimal systemic involvement while concurrently monitoring treatment efficacy. These therapies are particularly useful to the field of interventional oncology, where elevation of tumor drug levels, reduction of systemic side effects and post-therapy assessment are essential. This review highlights three such image-guided procedures: transarterial chemoembolization, drug-eluting implants and convection-enhanced delivery. Advancements in medical imaging technology have resulted in a growing number of new applications, including image-guided drug delivery. This minimally invasive approach provides a comprehensive answer to many challenges with local drug delivery. Future evolution of imaging devices, image-acquisition techniques and multifunctional delivery agents will lead to a paradigm shift in patient care.

The use of chemotherapy to treat cancer is a vital tool in cancer management but, due to several limiting factors such as the inherent risk of systemic toxicity and ineffective delivery to the diseased site, it is seldom used as a standalone treatment option [1]. Among the many strategies developed to overcome the inherent limitations of chemotherapy, no single approach can treat the many permutations of the disease. Instead, a variety of treatment regimens have been developed to treat specific types of cancer, with several strategies employing the use of local administration of therapeutic agents directly into the tumor. The local delivery of these agents has several advantages over systemic administration, including the ability to achieve very high local drug dosages, to avoid systemic side effects and to increase drug bioavailability by evading first-pass elimination. The ability to deliver chemotherapeutics locally, in a minimally invasive manner, has advanced drastically with the growth of medical imaging technologies.

Modern imaging techniques no longer focus solely on generating anatomical images, but instead are capable of performing a wide array of qualitative and quantitative tasks, ranging from monitoring physiological changes that occur in diseased tissues to assessing function at

[†]Author for correspondence: Tel.: +1 216 844 3544, agata.exner@case.edu.

Financial & competing interests disclosure

The authors have no relevant affiliations or financial involvement with any organization or entity with a financial interest in or financial conflict with the subject matter or materials discussed in the manuscript. This includes employment, consultancies, honoraria, stock ownership or options, expert testimony, grants or patents received or pending, or royalties. No writing assistance was utilized in the production of this manuscript.

a molecular level. These advances have not only helped diagnostic medicine, but have resulted in a new paradigm in drug delivery. The ability to guide or place devices in the body in a minimally invasive manner, noninvasively determine concentration and distribution of active agents and monitor treatment efficacy, sometimes performing all three with a single imaging modality, are paramount in providing feedback to both clinicians and researchers (Figure 1).

The advancements in medical imaging techniques have been particularly valuable in the field of interventional oncology, where a variety of imaging modalities are used to noninvasively evaluate the efficacy of therapeutic treatments through changes in tumor necrosis and vascularization [2–9]. Medical imaging has also led to the improvement of minimally invasive treatment options such as transarterial chemoembolization (TACE) and convection-enhanced delivery (CED). While the concepts of image-guided drug delivery can extend into the systemic delivery of contrast-enhanced particles and therapeutics, the focus of this review article will be on the local administration of therapeutics to solid tumors for interventional drug delivery, using image guidance for treatment planning and evaluation of treatment efficacy. This article will highlight advances in TACE, CED and implantable drug-eluting devices, as well as the intratumoral delivery of particle-based systems due to the role of medical imaging in directly accessing the tumor for interventional drug delivery.

Transarterial chemoembolization

The availability of high-speed real-time imaging modalities in combination with minimally invasive surgical techniques has led to the development of several local direct drug infusion protocols. One such minimally invasive image-guided local drug delivery procedure that has been commonly clinically employed is TACE. During this procedure a catheter is threaded into the local blood supply of a tumor under image guidance, a chemotherapeutic drug cocktail is administered directly to the tumor and an embolic agent is released to block blood flow. By selectively occluding the tumor blood supply, washout of the chemotherapeutic agent is prevented and higher drug dosages can be maintained within the tumor volume.

Transarterial chemoembolization is most often employed for treatment of hepatocellular carcinoma (HCC) in the liver; however, it has also been used for cholangiocarcinoma [10,11] and liver metastases [12,13]. Normal liver parenchyma is supplied by collateral portal venous and hepatic arterial circulation and receives two-thirds of its blood supply from the portal vein and one-third from hepatic arterial blood flow [14]. Meanwhile, hypervascular HCC tumors often receive much of their blood supply from the hepatic artery [14]. Therefore, embolotherapy blockage of peripheral hepatic arterial blood flow can initiate ischemic tumor necrosis, while leaving normal liver parenchyma intact as it is still supplied by collateral portal circulation [14,15]. TACE-treated HCC tumors that have greater portal involvement have a worse prognosis and have a greater chance for tumor recurrence than TACE-treated tumors with only hepatic arterial involvement [16]. While surgical resection is still the gold standard and preferred treatment option for HCC, this option is often not available due to commonly occurring concurrent cirrhotic liver disease, portal hypertension or poor hepatic reserve function, which are all associated with significant perioperative morbidity and mortality [15,17,18]. Consequently, minimally invasive

treatments such as TACE are often the only treatment options available for patients with HCC. Several randomized controlled trials have shown that TACE is a good therapeutic option for improving both patient survival and providing palliative therapy [19–22]. A recent cohort study by Miraglia *et al.* has shown that TACE is effective in achieving complete control of tumor growth in a majority of patients with a single HCC tumor less than 6 cm in diameter with complete tumor necrosis seen in 50–69% of cases [15]. On the other hand, the authors found that complete necrosis of HCC tumors greater than 6 cm was only achieved in 13% of patients [15].

Preprocedural imaging

Before TACE treatment can be undertaken, it is necessary to conduct baseline diagnostic imaging to determine tumor extent, as well as rule out any procedural contraindications such as portal-hepatic arterial shunts or portal vein thrombosis. Therefore, preprocedural evaluation using cross-sectional imaging modalities such as biphasic multidetector computed tomography (MDCT) or MRI is required (Figure 2A). In addition, digital subtraction angiography (DSA) of the celiac trunk must be conducted before injection of chemotherapeutic or embolic agents during the TACE procedure to determine the course of the tumor-feeding arteries (Figure 2B) [23]. Determining the correct tumor-feeding vessels is essential for selective positioning of the catheter during TACE to reduce collateral damage to normal liver parenchyma. Therefore, two imaging stations, one cross-sectional imaging modality such as MDCT or MRI to provide soft tissue information and one real-time fluoroscopy or DSA station to provide guidance for catheter placement, are necessary. Since transferring patients from one site to the other is inconvenient, hybrid CT/DSA [24] or MRI/DSA [25] suites have been employed over the past decade.

More recently, with the availability of digital flat-detector angiographic systems, a new class of C-arm CT imaging devices that can provide both conventional DSA and CT-like soft tissue images have been developed. C-arm CT data is obtained by rotating the flat-detector around a patient and obtaining multiplanar reconstruction images. Concurrent injection of contrast agent into the hepatic artery provides hemodynamic information. These C-arm CT devices have improved convenience due to a single machine providing all the required information, as well as greater sensitivity in detecting small hypervascular HCC lesions (<2 cm) than MDCT [26,27]. Compared with conventional DSA, C-arm CT has been shown to have significantly higher sensitivity, specificity and accuracy in finding tumor feeding arteries according to a study by Iwazawa *et al.* [23]. However, one limitation of these systems is the limited field of view, with a study by Meyer *et al.* showing that two-thirds of their cases had incomplete liver coverage using a medium sized flat-detector [26]. Therefore, preprocedural planning using flat-detecting MDCT is still recommended, but C-arm CT can be used exclusively during TACE treatment once a narrower tumor field of view has been established [23,26].

Embolic agents

A variety of embolic agents including polyvinyl alcohol (PVA) particles, gelatin sponges, autologous clots, steel coils and starch microspheres have been used to occlude vessels during TACE. PVA particles and steel coils are permanent embolic agents, while gelatin

sponges only temporarily occlude vessels. With the latter, revascularization occurs after several weeks. Due to their proven safety, gelatin sponges are the most widely used embolic agent [28]. In addition to the aforementioned agents, which perform the sole function of vascular occlusion, several other notable agents are multifunctional and act as occlusion agents and drug delivery vehicles. Of these, the most important is lipiodol, an iodinated ethyl ester of the fatty acids in poppy seed oil. Lipiodol selectively accumulates in tumor tissue due to a lack of Kupffer cells and can remain there for several weeks to a year after injection [29]. However, in normal liver parenchyma, lipiodol collects in portal venules where it is phagocytized by Kupffer cells and quickly cleared [29]. Lipiodol acts as a drug delivery vehicle due to its ability to carry and localize chemotherapeutic agents inside a tumor volume. To incorporate delivery capability, chemotherapeutic drugs, most commonly doxorubicin, 5-fluoruracil or cisplatin, are mixed with lipiodol until an emulsification is created. A study by Nakamura *et al.* has shown that when the ratio of lipiodol to drug solution is correctly adjusted, approximately 3:1 (lipiodol:doxorubicin) for their studies, drug is slowly released from the emulsion and pharmacokinetic outcomes are better than direct chemotherapeutic infusion [30]. It has also been shown that subsequent Gelfoam® embolization can also slow down release of drug from the lipiodol emulsion and prevents washout, resulting in increased drug concentration in the tumor volume [31]. As an embolic agent, lipiodol occludes microvessels and can reach portal veins around the tumor periphery through arterioportal communication routes [30]. Since tumors that have portal involvement are the most resistant to TACE, the ability of lipiodol to reach and accumulate in portal circulation surrounding a tumor can greatly strengthen anti-tumor effects [32]. Finally, since lipiodol is iodinized, it also acts as a CT contrast agent and its tumor accumulation can be examined postoperatively using CT [33].

Recently, another type of combination drug delivery–embolic agent, injection of controlled release chemotherapeutic drug-eluting beads (DEBs), has been developed and is currently undergoing clinical trials. Currently there are two types of drug-eluting microsphere-based systems available for TACE, DC Bead microspheres (Biocompatibles, UK) and Quadrasphere micropsheres (Biosphere Medical). The DC beads are comprised of a PVA polymer hydrogel with a sulfonic acid additive and can be polymerized into different sized microspheres from 100–900 μm [34]. These beads can be loaded with a variety of chemotherapeutic agents, with the two most common being doxorubicin and irinotecan, and have been shown to be effective in improving patient survival [35,36]. The Quadrasphere microspheres are the more recently developed of the two DEB systems and are comprised of hydrophilic, acrylic copolymer that can absorb up to 64 times its dry state volume [37]. These particles have a dry volume of 50–200 μm, which can expand to 200–800 μm [37]. While much less studied than PVA particles, recent studies have shown that Quadrasphere particles loaded with cisplatin or doxorubicin are promising for use with TACE therapy [38,39].

In comparison with traditional TACE with direct infusion or as an emulsion with lipiodol, the half-life of doxorubicin is greatly increased with PVA DEB and has been shown to range from 150–1730 h depending on bead size [40]. Therefore, the anti-tumor effect of DEB after TACE is prolonged and tumor necrosis can take place up to 40 days post-treatment [40]. Recent clinical studies have shown that DEB particles are more effective at improving

survival in patients with unresectable HCC tumors than traditional TACE embolic agents and many centers have shifted to using DEB particle-based TACE [40]. With the development of selective microcatheters to isolate tumor-feeding arteries and improvements in embolic agents the safety of this type of treatment has greatly increased. Recent trials have shown that severe complications, such as pulmonary embolism, are extremely rare with current treatment protocols. One study found that out of 1348 patients treated with a total of 2012 TACE procedures, there was only one case of pulmonary embolism, three cases of liver abscess and a very few other severe complications from TACE therapies [41].

Peri-operative imaging & treatment efficacy

After TACE treatment, proper follow up and assessment of treatment efficacy is vital. However, traditional measures of tumor response to therapy such as those outlined by the WHO and the response evaluation criteria in solid tumors (RECIST) do not correlate well with response to local percutaneous therapies such as TACE [19,22]. Tumors treated with TACE may have necrosis, edema or hemorrhage, which can have variable effects on tumor size, the primary criteria used for WHO and RECIST. For TACE, the European Association For Study of Liver criteria, which estimates the reduction in viable tumor volume through loss of tumor enhancement in imaging, is the preferred method of measuring tumor response to therapy [19,42]. Although loss of tumor enhancement does correlate well with tumor necrosis, the assessment of enhancement with CT can be difficult if the tumor is infused with lipiodol, which is radio-opaque (Figure 2D). Evaluation of tumor enhancement with MRI or contrast-enhanced ultrasound, however, is not affected by iodized oil and has been shown to correlate well to tumor necrosis when using the European Association for Study of Liver criteria [40,43]. While lipiodol obscures CT assessment of tumor enhancement, tumor uptake of lipiodol using noncontrast CT may itself also serve as marker for tumor necrosis (Figure 2C & D) [33,44,45]. Tumors that show homogenous accumulation of lipiodol are strongly correlated with necrosis on histopathology, while incomplete or spotty uptake of lipiodol is suggestive of a viable tumor [45].

In addition to quantifying tumor enhancement to assess treatment, functional imaging using CT, positron emission tomography (PET) and MRI can also be used to evaluate postoperative tumor necrosis. Diffusion-weighted MRI (DWI) measures the apparent diffusion coefficient (ADC), which detects the Brownian motion of water molecules in tissue. Water mobility in viable tumors is reduced due to the presence of intact cell membranes and results in a low ADC value. On the other hand, increased water diffusion and a high ADC value is correlated with tumor necrosis [43]. PET measures tumor viability by detecting radioactive decay of a glucose analog, fluorodeoxyglucose (^{18}F), to measure tumor metabolism. However, while PET is sensitive and has been used to measure tumor response to TACE therapy [46], it has poor spatial resolution and soft tissue contrast. Newer combined PET/CT imaging workstations may be more suitable for this application since they combine the high spatial resolution of CT and exquisite sensitivity of PET. CT perfusion imaging can also be used as an alternative to assess tumor response to therapy by measuring perfusion parameters pre- and post-treatment [47]. A study by Chen *et al.* demonstrated that tumors undergoing successful treatment had significantly decreased hepatic arterial perfusion, hepatic arterial fracture and hepatic blood volume perfection CT

parameters post-TACE treatment compared with pre-TACE, while the same perfusion parameters were insignificantly different for viable tumor groups [48].

Implantable drug-eluting devices

For tumors with collateral blood supply or shunting, TACE treatment may be ineffective or dangerous to surrounding parenchyma and other treatment strategies must be employed. One solution for treating these types of tumors is through the use of locally implanted chemotherapy-eluting implants. These implants are usually comprised of a biodegradable polymer matrix loaded with an active chemotherapeutic agent, which is slowly released over a period of several days to several weeks after implantation into a tumor. These implantable devices may be either a solid preformed implant or an *in situ*-forming implant (ISFI), which is initially in a liquid or gel phase and solidifies once injected into the body in response to different stimuli. Many of these implants can be placed into a tumor volume in a minimally invasive manner using image guidance and strategies to monitor or predict *in vivo* drug release using noninvasive imaging have been developed.

Preformed implants

Preformed implants are usually manufactured using extrusion or compression molding and can be designed to a variety of shapes and sizes. Since implant shape and surface area have a significant effect on drug release as well as implant degradation, the ability to control these design parameters results in more reproducible drug release. Several biodegradable polymers such as polyanhydrides, polyesters and poly(orthoesters) are used to formulate these drug delivery devices. In particular, implants comprised of poly(lactic acid) (PLA), poly(glycolic acid) (PGA) or their copolymer poly(lactic-co-glycolic acid) (PLGA) are especially common [49,50]. The biocompatibility, degradation and drug-release mechanisms from PLGA matrices have been well established [51,52]. In addition to the polymer, the other major component of these implants is the drug agent that is homogenously distributed within the implant matrix. For cancer drug delivery, a variety of chemotherapeutic agents, including cisplatin [53], carboplatin [54,55], doxorubicin [50], carmustine (BCNU) [56,57], 5-fluoruracil (5-FU) [58] and paclitaxel (PTX) [59] have been loaded into preformed controlled release implants. One such system that is currently in clinical use for treatment of malignant glioblastoma multiforme is comprised of a dime-sized polyanhydride wafer loaded with BCNU. The Gliadel® wafers (MGI Pharma, Inc., Bloomington, USA) are used to bypass the blood–brain barrier (BBB) and deliver high local doses of BCNU to treat residual tumor cells after surgical resection [60]. Currently, these implants are the only US FDA-approved preformed solid local drug delivery implants in clinical use.

While Gliadel wafers have been shown to be effective in the treatment of malignant brain tumors, their disk-like shape is unfavorable for minimally invasive placement into a tumor site using imaged-guided procedures. Another preformed implant device in the shape of a thin cylinder or ‘millirod’ formed by compression heat molding has been designed in particular for use with minimally invasive techniques and has been extensively studied. These implants are comprised of PLGA and have been developed as both sustained and dual release formulations [49,61]. Dual release millirods produce an initial burst of drug release

to quickly reach therapeutic drug dosage, followed by sustained release to maintain drug levels (Figure 3). The implants are formulated by dip coating the initial compressed PLGA millirod in polymer with NaCl or poly(ethylene oxide) to form a thin membrane, which quickly dissolves and releases drug when placed in an aqueous environment [49]. The shape of these implants was chosen so that they can be placed into a tumor volume using a custom percutaneous catheter under image guidance with CT, ultrasound or MRI. Animal studies have shown that these implants can be effective in the treatment of metastatic VX2 liver tumors in rabbits on their own or as adjuvant therapy post-radiofrequency ablation treatment [50,62].

In situ-forming implants

An ISFI consists of a liquid polymer solution that solidifies into a controlled release implant upon injection into a tissue environment. This process of solidification from liquid solution to solid implant can be initiated by a variety of stimuli such as water, temperature, pH changes or light [63]. Due to their injectable nature, these implants can be more easily placed in a tumor volume using image-guided percutaneous catheter-based methods than preformed implants. In addition, the manufacturing process for these implants is very mild and nondestructive and therefore, fragile drug molecules such as peptide based-therapies can be easily incorporated and released. A variety of responsive systems including hydrogels and thermoplastic pastes are utilized for ISFI formation. Thermoplastic pastes solidify upon a change in temperature and are comprised of a polymer melt that solidifies upon cooling to body temperature. Due to the need for low glass-transition temperatures (T_g) and low melting points (<60°C), polymers used for this application are often of low molecular weight. Thermoplastic pastes are often made from monomers of PLA, PGA, ε-caprolactone or orthoesters [63]. Several studies have shown that PTX- loaded thermoplastic ISFIs have been effective in treating and delivering chemotherapeutic agents to a local tumor site [59,64]. However, while these ISFI systems were able to sustain PTX release over a long time period (>60 days), drug release was very slow and the ability to reach therapeutic drug levels much beyond the implant borders was compromised [59]. Moreover, sustained subtherapeutic drug levels increases the chance of drug-resistance development (Figure 3B). One solution to increase the release rate of PTX from these ISFI pastes is to add water-soluble additives, such as gelatin or albumin [63].

In addition to thermoplastic pastes, ISFI systems that solidify upon injection into an aqueous environment are also a popular area of research in cancer drug delivery. These ISFIs initially consist of a solution of a biodegradable polymer such as PLGA or poly(ε-caprolactone) dissolved in an organic solvent such as *N*-methyl-2-pyrrolidone (NMP) [55,65], triacetin [66] or ethyl benzoate [67]. Upon injection into an aqueous environment, solvent will leach out of the polymer implant solution and water will influx in as the polymer matrix solidifies out of solution. The process by which this conversion from a liquid phase to a solid phase occurs is commonly referred to as phase inversion. The rate of implant phase inversion is highly dependent on the polymer type, as well as hydrophilicity of the organic solvent [67,68]. Drug molecules that are either suspended or dissolved in the polymer solution will also diffuse out of the implant in a controlled release manner. While these ISFI systems are often comprised of the same polymeric materials as preformed implants and have a similar

controlled release profile, the mechanisms of drug release from these systems are more complicated due to the phase inversion process. For example, the organic solvent properties play a considerable role in determining the drug release profile from these implants. Studies by McHugh *et al.* have shown that polymer solutions dissolved in relatively hydrophobic solvents, such as ethyl benzoate, display a zero order peptide drug release profile and classifies this group of ISFIs as slow phase-inverting systems [68]. On the other hand, polymer solutions comprised of a relatively hydrophilic solvent, such as NMP, exhibit a burst drug release profile similar to the previously described dual release millirods, whereby a large percentage of the loading drug dosage is released within the first day, followed by steady maintenance drug release [69]. In addition to solvent properties, excipient additives such as Pluronic surfactant [69], peptide molecules or triacetin have also been shown to affect the drug release profile from these implants. Moreover, certain excipient Pluronic surfactants, such as Pluronic P85 (P85), can have chemosensitizing effects on cancer cells to help overcome drug resistance. A study by Krupka *et al.* has shown that phase-inverting ISFIs with excipient P85 and loaded with carboplatin were more effective in treating ablated subcutaneous colorectal carcinoma tumors in rats than direct drug injection or implants without excipient [55].

Imaging implant formation & drug release

As described above, phase-inverting ISFIs solidify upon injection into an aqueous medium. Several studies have demonstrated that drug release from these types of ISFIs is directly correlated with implant precipitation or phase inversion [66,70]. Recently, imaging techniques using electron paramagnetic resonance (EPR) spectroscopy or ultrasound have been developed to image ISFIs *in vivo*. EPR examines the interaction of paramagnetic spin probes with their external environment to gain information about the microviscosity or spatial distribution of probes within the drug delivery implants. A study by Kempe *et al.* incorporated a nitroxyl spin probe, tempolbenzoate, into an NMP/PLGA ISFI and found the mobility of the spin probe to decrease as the implant precipitated [71]. Utilizing EPR imaging and correlating the spin probe signal to measured standards, the authors were able to monitor implant precipitation in both an *in vivo* and *in vitro* setting and found implant behavior to be similar in both [71]. More recently, another study by Solorio *et al.* demonstrated that ultrasound can be used to noninvasively monitor implant formation *in vitro* and *in vivo* [70]. Ultrasound imaging utilizes a piezoelectric transducer that converts mechanical pressure waves into an electrical signal and can record the backscatter that arises from impedance differences in a material. Since ISFIs undergo a process of phase inversion from a liquid polymer phase to a solid phase, this change of phase will alter the impedance of the implant material and can be detected by the ultrasound pressure waves (Figure 4). In contrast to the EPR finding of Kempe *et al.*, ultrasound studies demonstrated that *in vitro* and *in vivo* implant precipitation were significantly different [70,71]. Additionally, the authors were able to directly correlate drug release in each environment to implant precipitation [70].

While imaging phase inversion of ISFIs can be used to predict drug release, noninvasively monitoring *in vivo* drug release directly and subsequent tissue drug distribution would be much more beneficial. However, although several drug molecules have been tagged with

contrast agents for various imaging modalities, often the tag may alter the activity or mobility of these drugs and few studies to date have incorporated these types of molecules into drug delivery implants [72]. One study by Exner *et al.* that did directly monitor *in vivo* drug release and tissue distribution using CT utilized the high x-ray attenuation (Z = 78) of the heavy metal platinum in carboplatin-loaded millirods [54]. However, the authors concluded that, due to blurring artifacts and beam hardening from relatively high drug concentrations in the implant compared with the surrounding tissue, quantification of tissue drug concentrations using this method is difficult [54]. Additionally, the minimal drug dose detected by CT is quite high and lower therapeutic drug levels cannot be detected. Currently, while this method does provide some tissue drug distribution data, it is only accurate for measuring implant drug release.

Strategies to improve drug penetration

While drug-eluting implants can deliver very high local drug concentrations to a tumor site without avoiding systemic toxicity, relatively few of these devices have been translated for clinical use due to poor drug penetration into tissue. Typically, therapeutic tissue drug concentrations are only achieved a few millimeters away from the implant boundary [73]. Penetration and movement of drug into tissue is dependent on two tissue specific factors: drug diffusivity (*D*) and drug elimination, γ and can be described by the following first-order transport equation:

$$\frac{\partial C\,(r.t)}{\partial t} = D\nabla^2 C\,(r.t) - \gamma C\,(r.t)$$

where *C(r.t)* is the tissue drug concentration, *t* the time and ∇ the gradient operator. Therefore, to improve drug penetration from the implant boundary, either the tissue permeability must be increased, by increasing D, or the tissue drug elimination must be reduced by decreasing γ. One strategy to both increase tumor drug permeability and reduce drug elimination is to induce tissue necrosis. Cell membranes in necrotic tissue are usually destroyed and greater drug diffusivity has been shown to occur in these types of tissues [73]. Additionally, dead cells are metabolically inactive and tissue vasculature is often destroyed with necrosis, thereby eliminating the major routes of drug elimination from the tissue. Both ablative tumor treatments, as well as chemotherapy-induced tumor necrosis, have been shown to increase drug penetration [73,74].

In addition to inducing tumor necrosis, several other strategies have also been developed to improve drug penetration in tumors. One such strategy is to bind the drug molecule to a large molecular weight carrier that is not easily eliminated from the tissue. A study by Dang *et al.* demonstrated that methotrexate (MTX) that was covalently bonded to dextran was able to retain its cytotoxic activity while reducing tissue drug elimination [75]. Although the diffusivity of the larger molecular weight MTX-dextran molecule was lower, the reduction in tissue elimination was more than able to offset that factor and significant gains in tissue penetration were achieved [75]. Yet, although this is a promising strategy to increase tumor drug penetration, it can only be used for chemotherapeutic agents that act on surface receptors, such as MTX, which acts on cell surface folate receptors. Many commonly used

chemotherapeutic agents such as cisplatin, BCNU, PTX and doxorubicin work on intracellular targets that would become inaccessible if they are attached to a dextran carrier. Finally, if tissue-specific elimination and drug diffusivity properties are known, a study by Weinberg *et al.* has shown that a mathematical modeling approach to place multiple implants within a tumor volume can be used to achieve complete penetration [76]. Using this type of method, a patient-specific treatment approach can be designed by reconstructing 3D CT or MRI data of a tumor and using mathematical modeling to determine the number and location of implants to be placed in a tumor to achieve therapeutic levels throughout the volume [76]. However, while this method shows great promise, accurate tissue-specific diffusivity and elimination parameters may be difficult to obtain due to tumor tissue and anatomical variability. One solution to help overcome this barrier is the development of imaging contrast-tagged drug agents, whose tissue distributions can be non-invasively monitored to establish tissue-specific drug transport parameters.

Convection-enhanced delivery

Treatment of neuro-oncologic conditions has proven to be extremely difficult, due in part to the physiological and anatomical protection provided by the BBB. The BBB protects the CNS by limiting the passage of molecules from the circulating blood into the cerebrospinal fluid and interstitial fluid in the parenchyma, preventing the transport of many potentially potent therapeutic agents to the disease site [77]. In order to circumvent this naturally existing barrier, several researchers have focused on developing ways to disrupt the BBB. One such technique is opening the BBB by shrinking the endothelial cells of the BBB with an osmotically active solution resulting in an increased permeability of inter-endothelial tight junctions [78,79]. This effect is largely reversed after 10 min [79]. Another technique for BBB disruption includes the use of focused ultrasound with ultrasound contrast agents under MRI guidance [4,80,81]. This technique has shown that the BBB can be disrupted for as long as 4 h and allow molecules larger than 100 kDa to pass into the CNS [4,80,81]. While these techniques have shown some promise in the field of neuro-oncology [80,82], they are limited to treatment regions near vascular beds [83]. Additionally, other diffusion-based treatments such as polymeric devices and drug-pumping catheters can be surgically placed in a resected tumor bed [56,84], but the spatial distribution is limited by the diffusion distance of the drug (millimeter). Therefore, additional surgeries may be necessary if an increased dosage is required [83,85]. While all of these technologies provide a means by which drugs can be administered to the CNS, they are all limited by the low, nonhomogenous, distribution volumes that are the inherent shortcomings of diffusion-based delivery systems [83,85–87].

To improve CNS drug penetration beyond diffusional limitations, convective drug-delivery methods were developed. CED is a direct intracerebral means of drug delivery performed by sterotactically placing a cannula into the targeted region and maintaining a continuous pressure gradient to convectively deliver therapeutic agents through the extracellular space to a large tissue volume. CED has been shown to be a promising means of delivering drugs to treat a wide variety of illnesses from Parkinson’s disease (PD) to malignant gliomas [84,88–90]. In CED, because the distribution volume (V_d) is generated by the convective movement of the infusate, the drug is more homogenously distributed than diffusion-based

systems and the molecular weight of the drug plays a less significant role in the mass transport (Figure 5). Initially, this technique was limited by drug reflux along the cannula, due in part to improper infusion rates and poor cannula designs (Figure 5B). Ultimately, reflux results in a poor drug distribution within the tissue and, at times, can even lead to the leakage of drug from the target region into the CSF, potentially leading to systemic toxicities [83].

As imaging techniques have increased in sophistication, the insight gained has led to advances in not only cannula design, but in the role that the tissue properties play in the drug distribution volume [83,86,91,92]. The use of gadolinium-conjugated forms of albumin (Gd–albumin) has been especially instrumental in developing real-time imaging techniques of CED in the brain stem [88,93–95]. An interesting aspect of these studies was that the spatial distribution of larger molecular weight drugs could be correlated with the V_d of Gd–albumin (72 kDa) [95]. In a study evaluating the distribution of drug in rat and primate models, there was a 4.8% mean difference in the V_d between drug agent ^{125}I-IL-13 bound to *Pseudomonas* and Gd–albumin, which correlated to less than a 200-μm difference in the diameters of the V_d occupied by the surrogate tracer and the transported drug [95]. More recently, Gd–albumin was used to determine the effects of tissue properties on the spatial distribution of infused drug in the hypothalamus and hippocampus in rat models using high-resolution MRI (11.1 Tesla) [88]. When CED was used to deliver Gd–albumin to the hypothalamus, it was shown that regions with dense cell layers such as the dentate gyrus served as convective barriers for mass transport appearing as hypointense regions within the hypothalamus. It was hypothesized that, due to the decreased hydraulic conductance in these dense cell layers, the drug would flow around these structures into regions of higher conductivity, resulting in elevated concentrations in the less densely packed regions of the hypothalamus, highlighting the effect of neuroanatomy on the spatial distribution of drug within a region [88].

While Gd–albumin works well as a surrogate tracer for the real-time imaging of drugs with larger molecular weight, under conditions of low flow rates (<0.5 μl/min) or with infusion volumes greater than 2 ml, the distribution of smaller molecular weight drugs is more accurately determined using a Gd–diethylenetriamene pentaacetic acid (Gd–DTPA, molecular weight of 938 Da) tracer due to the importance of diffusion in the mass transport of the drug. This surrogate tracer system has been successfully used in the treatment of Gaucher disease in human patients [94,96,97]. While the use of surrogate tracers facilitate the real-time evaluation of drug dispersion and flow parameters that ensure proper drug dispersion, the ability to evaluate the spatial distribution of the actual drug in real time could prove to be paramount in designing optimal treatment regimens, such as iodine for synchrotron stereotactic radiotherapy or Gd in neutron capture therapy (NCT) [87]. In NCT a stable form of Gd or boron is delivered to tumors and upon irradiation with thermal or epithermal neutrons, γ-rays and auger electrons are released by the delivered Gd compounds [98–103]. The γ-rays and auger electrons that are emitted cause oxidative damage to DNA that ultimately result in cell necrosis if the Gd is extremely close to the DNA (0–150 nm) [99]. Boron treatments are typically used due to higher tumor uptake than Gd, resulting in a more effective tumor treatment [98,99,101,102]. Owing to a more complete understanding of the time-dependent intranuclear localization of Gd-based compounds and the ability to

see the spatial distribution using MRI, interest in Gd-based therapies has been reinvigorated [99]. Due to the increased time required for high levels of Gd to be taken in by cells, methods for increasing the retention time of Gd in tumors is being investigated [101]. In addition, advances in material chemistry that improve the cellular uptake of Gd may play a significant role in NCT in the future.

While it is clear that tissue properties play a critical role in the distribution of drug when using CED [84,91,93], cannula design and placement have been shown to be equally significant factors in limiting reflux and facilitating efficient distribution of drugs [83,86,92,93,104,105]. It has been demonstrated that cannulas with a novel step design – a regular cannula encased by a silicone outer layer – decrease reflux and have been adapted for use in nonhuman primates as well as for study in rats [83,92,105]. In both nonhuman primates and rats, there was a reduction in reflux and increasing V_d. This cannula design also facilitated an increase in both the rate and volume of infusion [83,92]. One interesting side effect of increased infusion volumes is that ventricular compression begins to occur in both nonhuman primate and canine models. In this case, ventricular compression does not appear to result in neurological symptoms and appears to only be temporary, but is important to monitor for the development of a safe delivery methodology [106]. When investigating the effects of cannula placement for preoperative planning, a recent study by Yin *et al.* showed that the distance of the cannula to white matter tracts, which serve as leakage points, appeared to be the most important factor in controlling the V_d during CED [92]. The primary target for treatment of PD has been the putamen [92]. In order to obtain a clinically relevant response from CED-based treatments, the distribution of the drug must be optimized [92]. In nonhuman primates, when cannulas were placed too close to the white matter tracts of the corpus callosum, internal capsule or the external capsule, significant leakage occurred, resulting in the loss of drug into the CSF [92,104,105,107]. The resultant images obtained from the study were analyzed to establish zones based on the distance from the white matter structures that could be used to limit leakage into the CSF and provide a 3D coordinate system for surgical planning in human patients for treating neurodegenerative diseases such as PD, as well as neuro-oncological treatments [92].

Advances in preoperative stereotactic planning [91,92,105], as well as the ability to visualize the V_d, may lead to more precise placement of the cannula, resulting in optimized treatment of nonresectable gliomas. Despite these advances, owing to the high level of expertise required for clinicians to successfully administer therapeutics via CED [108], as well as the high cost and exposure limitations inherent in MRI and CT [109], widespread use of the technique is currently limited.

Additional particle-based drug delivery approaches in TACE & CED

Particle-based delivery has been used to fill a diverse number of roles in the field of drug delivery and tissue engineering. One advantage to particles over other delivery systems is the ability to create particle suspensions that can be administered directly to the diseased region without exacerbating the injury with invasive surgery. In addition, in comparison with larger implant-based drug-delivery systems, smaller particle-based therapies can achieve greater tissue penetration, which in turn maximizes the treatment volume. When used for local drug

delivery, although the systemic dose is small, because drug is released in close proximity to the diseased tissue, high drug doses can be achieved in the target tissue, increasing the overall impact of the therapeutic agent that is released. Moreover, particles can be modified for systemic delivery [8,110,111], as well as injected directly into tumors, providing a means to treat metastatic disease [12,112–114]. These injectable particles provide a platform by which targeting moieties and contrast agents can be covalently attached without adversely affecting the drug, in addition to providing a platform for developing novel chemical formulations to control the drug-release kinetics. For these reasons and many others, particle-based therapies have found success in a variety of different treatment modalities from TACE to facilitating real-time imaging in CED.

One unique form of a particle-based therapy utilizes radioactive pharmaceuticals embedded in glass beads or resin-coated particles [115]. The use of radiopharmaceutics in a modified form of TACE, known as radioembolization, is a promising technique for treating nonresectable hepatic carcinomas. In order to insure optimal treatments, radioembolization requires blood flow and perfusion to maximize the therapeutic effect of the treatment. In this therapy, administration of radiopharmaceuticals such as yttrium-90 (^{90}Y) or rhenium-188 (^{188}Re) particles results in a high internal tumoricidal radiation source (up to 4993 Gy), which, when delivered to a targeted area, reduces the risk of causing radiation-induced liver disease and can be imaged using SPECT-CT [9,115–118]. However, while radiopharmaceuticals have been demonstrated to be effective in improving survival in patients with unresectable HCC tumors, few studies have compared them to more traditional TACE embolic agents and further studies are required.

Liposomes have played a critical role in the development of real-time CED and provide an optimal means of delivering chemotherapeutics such as PTX or topotecan for treating malignant gliomas, as well as protein-based therapies for treatment of PD [107,119,120]. Through the use of gadoteridol-labeled neutral liposomes, the convective process can be visualized in real time with MRI, while simultaneously maximizing the contact time of the treatment within the V_d [83]. The ability to visualize the liposome distribution during CED was important in establishing the role of reflux on the V_d, showing that once reflux begins, the relationship of infusion volume (Vi) to V_d does not change [83,104]. The result of this reflux-induced plateau is that drug is no longer being distributed within the target tissue, despite continued infusion, resulting in the leakage of drug to remote regions of the brain and possibly into the CSF [104]. While CED is designed to reduce the effects of molecular weight on drug distribution, the surface properties and size of the liposomes being delivered have been shown to play a role in their V_d [119,121]. When evaluating the effect of charge on the distribution of particles, it was demonstrated that neutral and anionic liposomes occupied a similar V_d, which was markedly different from the reduced distribution of cationic particles, most likely due to complex formation with the proteglycans of the extracellular matrix [121]. Steric shielding by PEG was shown to increase the tissue penetration for both neutral and anionic liposomes, but did not effectively increase penetration distance with cationic liposomes [121]. Finally, liposome size appears to play only a limited role in effecting the V_d. While liposomes have a smaller V_d than molecules such as dextran, the V_d of liposomes is relatively constant until the liposome diameter approaches 200 nm, at which point the V_d begins to decrease [121]. The ability to monitor

the convective delivery of therapeutic agents in real time is instrumental in insuring that the treatment volume is adequate [104]. In addition, understanding the effect of surface properties on the mass-transport behavior of particles is important for the improvement of software designed to aid in preoperative planning for this procedure.

Future perspective

Medical imaging is rapidly transforming patient care by providing safe, fast and reliable techniques that allow care providers to minimize the invasive nature of many therapeutic procedures (Table 1). One relatively novel field that imaging is now gaining ground in is drug delivery. Image-guided drug delivery has great potential to revolutionize patient care by facilitating a number of related processes, such as minimally invasive placement of drug-eluting devices into nonresectable tumors or noninvasive monitoring of therapeutic efficacy. Constant, rapid development of improved imaging modalities such as C-arm CT imaging has made it possible to more accurately select appropriate feeding arteries for microcatheter placement in TACE to enhance treatment efficacy, while concurrently reducing the probability of toxic side effects [26,27]. MRI advancements have not only provided a means for real-time imaging of the distribution volume of drugs and nanoparticles, but these innovations have also improved the reliability of CED as a neuro-oncological treatment option [83]. In addition, functional DWI is proving to be a reliable method by which one can monitor the necrosis of tumors after a variety of interventional treatments. As the field of image-guided drug delivery evolves, surgical procedures will not be performed without advanced modeling and planning based on preoperative imaging. One example would be the use of MRI to determine the 3D coordinates of the optimal placement of a cannula in order to avoid reflux into the CSF during a CED procedure. Improvements in functional imaging may also be used to develop feedback systems so that therapeutic planning can be adjusted and tailored for more personalized treatment.

While image-guided drug delivery in clinical settings is ever growing, the role of imaging in research is becoming equally valuable. The development of imaging techniques to provide high-throughput noninvasive methods of monitoring drug delivery and treatment efficacy is a key factor in developing screening methods in industrial and laboratory settings. The use of molecular-imaging techniques will provide a means of diagnosing conditions and will also be used for targeted drug delivery. It may even lead to nontoxic treatment options through the development of prodrug-based therapies. In addition to advances in targeted drug delivery, research in image-guided drug delivery will play a key role in developing theranostic multifunctional agents, which will provide a means to not only personalize the treatment, but concurrently provide a noninvasive means for evaluating its efficacy.

Bibliography

Papers of special note have been highlighted as:

■■ of considerable interest

1. Exner AA, Saidel GM. Drug-eluting polymer implants in cancer therapy. Expert Opin Drug Deliv. 2008; 5(7):775–788. [PubMed: 18590462]
2. Fass L. Imaging and cancer: a review. Mol Oncol. 2008; 2(2):115–152. [PubMed: 19383333]

3. Hong K, Georgiades CS, Geschwind JF. Technology insight: image-guided therapies for hepatocellular carcinoma–intra-arterial and ablative techniques. Nat Clin Pract Oncol. 2006; 3(6): 315–324. [PubMed: 16757969]
4. Kinoshita M, Mcdannold N, Jolesz FA, Hynynen K. Noninvasive localized delivery of herceptin to the mouse brain by MRI-guided focused ultrasound- induced blood-brain barrier disruption. Proc Natl Acad Sci USA. 2006; 103(31):11719–11723. [PubMed: 16868082]
5. Korpanty G, Carbon JG, Grayburn PA, Fleming JB, Brekken RA. Monitoring response to anticancer therapy by targeting microbubbles to tumor vasculature. Clin Cancer Res. 2007; 13(1):323–330. [PubMed: 17200371]
6. Kruskal JB, Goldberg SN. Emerging therapies for hepatocellular carcinoma: opportunities for radiologists. J Vasc Interv Radiol. 2002; 13(9 Pt 2):S253–258. [PubMed: 12354843]
7. Lee DJ, Lyshchik A, Huamani J, Hallahan DE, Fleischer AC. Relationship between retention of a vascular endothelial growth factor receptor 2 (VEGFR2)-targeted ultrasonographic contrast agent and the level of VEGFR2 expression in an *in vivo* breast cancer model. J Ultrasound Med. 2008; 27(6):855–866. [PubMed: 18499845]
8. Lu ZR, Ye F, Vaidya A. Polymer platforms for drug delivery and biomedical imaging. J Control Release. 2007; 122(3):269–277. [PubMed: 17662500]
9. Vossen JA, Buijs M, Kamel IR. Assessment of tumor response on MR imaging after locoregional therapy. Tech Vasc Interv Radiol. 2006; 9(3):125–132. [PubMed: 17561215]
10. Gusani NJ, Balaa FK, Steel JL, et al. Treatment of unresectable cholangiocarcinoma with gemcitabine-based transcatheter arterial chemoembolization (TACE). A single-institution experience. J Gastrointest Surg. 2008; 12(1):129–137. [PubMed: 17851723]
11. Herber S, Otto G, Schneider J, et al. Transarterial chemoembolization (TACE) for inoperable intrahepatic cholangiocarcinoma. Cardiovasc Intervent Radiol. 2007; 30(6):1156–1165. [PubMed: 17508242]
12. Al-Ghananeem AM, Malkawi AH, Muammer YM, et al. Intratumoral delivery of paclitaxel in solid tumor from biodegradable hyaluronan nanoparticle formulations. AAPS Pharm Sci Tech. 2009; 10(2):410–417.
13. Huppert PE, Fierlbeck G, Pereira P, et al. Transarterial chemoembolization of liver metastases in patients with uveal melanoma. Eur J Radiol. 2009; 74(3):E38–E44. [PubMed: 19467811]
14. Breedis C, Young G. The blood supply of neoplasms in the liver. Am J Pathol. 1954; 30(5):969–977. [PubMed: 13197542]
15. Miraglia R, Pietrosi G, Maruzzelli L, et al. Efficacy of transcatheter embolization/chemoembolization (TAE/TACE) for the treatment of single hepatocellular carcinoma. World J Gastroenterol. 2007; 13(21):2952–2955. [PubMed: 17589945]
16. Shirabe K, Kajiyama K, Harimoto N, et al. Prognosis of hepatocellular carcinoma accompanied by microscopic portal vein invasion. World J Gastroenterol. 2009; 15(21):2632–2637. [PubMed: 19496194]
17. Benzoni E, Molaro R, Cedolini C, et al. Liver resection for HCC: analysis of causes and risk factors linked to postoperative complications. Hepatogastroenterology. 2007; 54(73):186–189. [PubMed: 17419257]
18. Teh SH, Christein J, Donohue J, et al. Hepatic resection of hepatocellular carcinoma in patients with cirrhosis: model of end-stage liver disease (MELD) score predicts perioperative mortality. J Gastrointest Surg. 2005; 9(9):1207–1215. [PubMed: 16332475]
19. Bruix J, Lovet JM, Castells A, et al. Transarterial embolization versus symptomatic treatment in patients with advanced hepatocellular carcinoma: results of a randomized, controlled trial in a single institution. Hepatology. 1998; 27(6):1578–1583. [PubMed: 9620330]
20. Lin DY, Liaw YF, Lee TY, Lai CM. Hepatic arterial embolization in patients with unresectable hepatocellular carcinoma – a randomized controlled trial. Gastroenterology. 1988; 94(2):453–456. [PubMed: 2826285]
21. Lo CM, Ngan H, Tso Wk, et al. Randomized controlled trial of transarterial lipiodol chemoembolization for unresectable hepatocellular carcinoma. Hepatology. 2002; 35(5):1164–1171. [PubMed: 11981766]

22■■. Takayasu K, Arii S, Ikai I, et al. Overall survival after transarterial lipiodol infusion chemotherapy with or without embolization for unresectable hepatocellular carcinoma: propensity score analysis. AJR Am J Roentgenol. 2010; 194(3):830–837. Demonstrated that transarterial chemoembolization was associated with significantly better overall survival rates than transarterial infusion therapy without embolization in patients with unresectable hepatocellular carcinoma. [PubMed: 20173167]

23. Iwazawa J, Ohue S, Mitani T, et al. Identifying feeding arteries during tace of hepatic tumors: comparison of c-arm CT and digital subtraction angiography. AJR Am J Roentgenol. 2009; 192(4):1057–1063. [PubMed: 19304714]

24. Murakami T, Oi H, Hori M, et al. CT arterial portography and CT arteriography with a triple-lumen balloon catheter. Acta Radiol. 1997; 38(4 Pt 1):553–557. [PubMed: 9240677]

25. Vogl TJ, Balzer JO, Mack MG, Bett G, Oppelt A. Hybrid MR interventional imaging system: combined MR and angiography suites with single interactive table. Feasibility study in vascular liver tumor procedures. Eur Radiol. 2002; 12(6):1394–1400. [PubMed: 12042944]

26. Meyer BC, Frericks BB, Voges M, et al. Visualization of hypervascular liver lesions during TACE: comparison of angiographic C-arm CT and MDCT. AJR Am J Roentgenol. 2008; 190(4):W263–W269. [PubMed: 18356419]

27. Valls C, Cos M, Figueras J, et al. Pretransplantation diagnosis and staging of hepatocellular carcinoma in patients with cirrhosis: value of dual-phase helical CT. AJR Am J Roentgenol. 2004; 182(4):1011–1017. [PubMed: 15039179]

28. Coldwell DM, Stokes KR, Yakes WF. Embolotherapy: agents, clinical applications and techniques. Radiographics. 1994; 14(3):623–643. quiz 645–626. [PubMed: 8066276]

29. Kan Z, Mccuskey PA, Wright KC, Wallace S. Role of Kupffer cells in iodized oil embolization. Invest Radiol. 1994; 29(11):990–993. [PubMed: 7890514]

30. Nakamura H, Hashimoto T, Oi H, Sawada S. Iodized oil in the portal vein after arterial embolization. Radiology. 1988; 167(2):415–417. [PubMed: 2833765]

31. Raoul JL, Heresbach D, Bretagne JF, et al. Chemoembolization of hepatocellular carcinomas. A study of the biodistribution and pharmacokinetics of doxorubicin. Cancer. 1992; 70(3):585–590. [PubMed: 1320447]

32. Sasaki Y, Imaoka S, Kasugai H, et al. A new approach to chemoembolization therapy for hepatoma using ethiodized oil, cisplatin and gelatin sponge. Cancer. 1987; 60(6):1194–1203. [PubMed: 2441837]

33. Jeon UB, Lee JW, Choo KS, et al. Iodized oil uptake assessment with cone-beam CT in chemoembolization of small hepatocellular carcinomas. World J Gastroenterol. 2009; 15(46): 5833–5837. [PubMed: 19998505]

34. Liapi E, Geschwind JF. Intra-arterial therapies for hepatocellular carcinoma: where do we stand? Ann Surg Oncol. 2010; 17(5):1234–1246. [PubMed: 20405328]

35. Martin RC, Robbins K, Tomalty D, et al. Transarterial chemoembolisation (TACE) using irinotecan-loaded beads for the treatment of unresectable metastases to the liver in patients with colorectal cancer: an interim report. World J Surg Oncol. 2009; 7:80. [PubMed: 19886993]

36. Malagari K, Pomoni M, Kelekis A, et al. Prospective randomized comparison of chemoembolization with doxorubicin-eluting beads and bland embolization with beadblock for hepatocellular carcinoma. Cardiovasc Intervent Radiol. 2010; 33(3):541–551. [PubMed: 19937027]

37. Liapi E, Geschwind JF. Transcatheter and ablative therapeutic approaches for solid malignancies. J Clin Oncol. 2007; 25(8):978–986. [PubMed: 17350947]

38. De Luis E, Bilbao JI, De Ciercoles JA, et al. *In vivo* evaluation of a new embolic spherical particle (hepasphere) in a kidney animal model. Cardiovasc Intervent Radiol. 2008; 31(2):367–376. [PubMed: 18167024]

39. Poggi G, Quaretti P, Minoia C, et al. Transhepatic arterial chemoembolization with oxaliplatin-eluting microspheres (OEM-TACE) for unresectable hepatic tumors. Anticancer Res. 2008; 28(6B):3835–3842. [PubMed: 19192637]

40. Moschouris H, Malagari K, Papadaki MG, Kornezos I, Matsaidonis D. Contrast-enhanced ultrasonography of hepatocellular carcinoma after chemoembolisation using drug-eluting beads: a

pilot study focused on sustained tumor necrosis. Cardiovasc Intervent Radiol. 2010 (Epub ahead of print).

41. Xia J, Ren Z, Ye S, et al. Study of severe and rare complications of transarterial chemoembolization (TACE) for liver cancer. Eur J Radiol. 2006; 59(3):407–412. [PubMed: 16621394]
42. Malagari K, Chatzimichael K, Alexopoulou E, et al. Transarterial chemoembolization of unresectable hepatocellular carcinoma with drug eluting beads: results of an open-label study of 62 patients. Cardiovasc Intervent Radiol. 2008; 31(2):269–280. [PubMed: 17999110]
43. Kamel IR, Bluemke DA, Eng J, et al. The role of functional MR imaging in the assessment of tumor response after chemoembolization in patients with hepatocellular carcinoma. J Vasc Interv Radiol. 2006; 17(3):505–512. [PubMed: 16567675]
44. Brown DB, Gould JE, Gervais DA, et al. Transcatheter therapy for hepatic malignancy: standardization of terminology and reporting criteria. J Vasc Interv Radiol. 2007; 18(12):1469–1478. [PubMed: 18057279]
45. Lim HK, Han JK. Hepatocellular carcinoma: evaluation of therapeutic response to interventional procedures. Abdom Imaging. 2002; 27(2):168–179. [PubMed: 11847576]
46. Vitola JV, Delbeke D, Meranze SG, Mazer MJ, Pinson CW. Positron emission tomography with f-18-fluorodeoxyglucose to evaluate the results of hepatic chemoembolization. Cancer. 1996; 78(10):2216–2222. [PubMed: 8918417]
47. Lin WY, Wang SJ, Yeh SH. Hepatic perfusion index in evaluating treatment effect of transcatheter hepatic artery embolization in patients with hepatocellular carcinoma. Neoplasma. 1995; 42(2):89–92. [PubMed: 7617083]
48. Chen G, Ma DQ, He W, Zhang BF, Zhao LQ. Computed tomography perfusion in evaluating the therapeutic effect of transarterial chemoembolization for hepatocellular carcinoma. World J Gastroenterol. 2008; 14(37):5738–5743. [PubMed: 18837093]
49. Qian F, Szymanski A, Gao J. Fabrication and characterization of controlled release poly(D,L-lactide-co-glycolide) millirods. J Biomed Mater Res. 2001; 55(4):512–522. [PubMed: 11288079]
50. Weinberg BD, Blanco E, Lempka SF, Anderson JM, Exner AA, Gao J. Combined radiofrequency ablation and doxorubicin-eluting polymer implants for liver cancer treatment. J Biomed Mater Res A. 2007; 81(1):205–213. [PubMed: 17120205]
51. Athanasiou KA, Niederauer GG, Agrawal CM. Sterilization, toxicity, biocompatibility and clinical applications of polylactic acid/polyglycolic acid copolymers. Biomaterials. 1996; 17(2):93–102. [PubMed: 8624401]
52. Jain RA. The manufacturing techniques of various drug loaded biodegradable poly(lactide-co-glycolide) (PLGA) devices. Biomaterials. 2000; 21(23):2475–2490. [PubMed: 11055295]
53. Chen FA, Kuriakose MA, Zhou MX, Delacure MD, Dunn Rl. Biodegradable polymer-mediated intratumoral delivery of cisplatin for treatment of human head and neck squamous cell carcinoma in a chimeric mouse model. Head Neck. 2003; 25(7):554–560. [PubMed: 12808659]
54. Exner AA, Weinberg BD, Stowe NT, et al. Quantitative computed tomography analysis of local chemotherapy in liver tissue after radiofrequency ablation. Acad Radiol. 2004; 11(12):1326–1336. [PubMed: 15596370]
55. Krupka TM, Weinberg BD, Ziats NP, Haaga JR, Exner AA. Injectable polymer depot combined with radiofrequency ablation for treatment of experimental carcinoma in rat. Invest Radiol. 2006; 41(12):890–897. [PubMed: 17099428]
56. Brem H, Gabikian P. Biodegradable polymer implants to treat brain tumors. J Control Release. 2001; 74(1–3):63–67. [PubMed: 11489483]
57. Fleming AB, Saltzman WM. Pharmacokinetics of the carmustine implant. Clin Pharmacokinet. 2002; 41(6):403–419. [PubMed: 12074689]
58. Haaga JR, Exner AA, Wang Y, Stowe NT, Tarcha PJ. Combined tumor therapy by using radiofrequency ablation and 5-FU-laden polymer implants. Evaluation in rats and rabbits. Radiology. 2005; 237(3):911–918. [PubMed: 16237145]
59. Walter KA, Cahan MA, Gur A, et al. Interstitial taxol delivered from a biodegradable polymer implant against experimental malignant glioma. Cancer Res. 1994; 54(8):2207–2212. [PubMed: 7909720]

60. Wang CC, Li J, Teo CS, Lee T. The delivery of BCNU to brain tumors. J Control Release. 1999; 61(1–2):21–41. [PubMed: 10469900]

61. Qian F, Nasongkla N, Gao J. Membrane-encased polymer millirods for sustained release of 5-fluorouracil. J Biomed Mater Res. 2002; 61(2):203–211. [PubMed: 12007200]

62. Weinberg BD, Ai H, Blanco E, Anderson JM, Gao J. Antitumor efficacy and local distribution of doxorubicin via intratumoral delivery from polymer millirods. J Biomed Mater Res A. 2007; 81(1):161–170. [PubMed: 17120197]

63. Hatefi A, Amsden B. Biodegradable injectable *in situ* forming drug delivery systems. J Control Release. 2002; 80(1–3):9–28. [PubMed: 11943384]

64. Jackson JK, Gleave ME, Yago V, Beraldi E, Hunter Wl, Burt HM. The suppression of human prostate tumor growth in mice by the intratumoral injection of a slow-release polymeric paste formulation of paclitaxel. Cancer Res. 2000; 60(15):4146–4151. [PubMed: 10945622]

65. Patel RB, Carlson AN, Solorio L, Exner AA. Characterization of formulation parameters affecting low molecular weight drug release from *in situ* forming drug delivery systems. J Biomed Mater Res A. 2010; 94(2):476–484. [PubMed: 20186771]

66. Graham PD, Brodbeck KJ, McHugh AJ. Phase inversion dynamics of PLGA solutions related to drug delivery. J Control Release. 1999; 58(2):233–245. [PubMed: 10053196]

67. Brodbeck KJ, Desnoyer JR, McHugh AJ. Phase inversion dynamics of PLGA solutions related to drug delivery. Part ii. The role of solution thermodynamics and bath-side mass transfer. J Control Release. 1999; 62(3):333–344. [PubMed: 10528071]

68. McHugh AJ. The role of polymer membrane formation in sustained release drug delivery systems. J Control Release. 2005; 109(1–3):211–221. [PubMed: 16288815]

69. Desnoyer JR, Mchugh AJ. The effect of pluronic on the protein release kinetics of an injectable drug delivery system. J Control Release. 2003; 86(1):15–24. [PubMed: 12490369]

70■■. Solorio L, Babin BM, Patel RB, Mach J, Azar N, Exner AA. Noninvasive characterization of *in situ* forming implants using diagnostic ultrasound. J Control Release. 2010; 143(2):183–190. Demonstrated that ultrasound could be used to visualize the behavior of *in situ*-forming polymer implants *in vivo*, with a linear correlation between drug release and phase inversion. [PubMed: 20060859]

71. Kempe S, Metz H, Pereira PG, Mader K. Noninvasive *in vivo* evaluation of *in situ* forming PLGA implants by benchtop magnetic resonance imaging (BT-MRI) and EPR spectroscopy. Eur J Pharm Biopharm. 2010; 74(1):102–10. [PubMed: 19545625]

72. Weinberg BD, Blanco E, Gao J. Polymer implants for intratumoral drug delivery and cancer therapy. J Pharm Sci. 2008; 97(5):1681–1702. [PubMed: 17847077]

73. Weinberg BD, Patel RB, Exner AA, Saidel GM, Gao J. Modeling doxorubicin transport to improve intratumoral drug delivery to RF ablated tumors. J Control Release. 2007; 124(1–2):11–19. [PubMed: 17900740]

74. Au JL, Jang SH, Zheng J, et al. Determinants of drug delivery and transport to solid tumors. J Control Release. 2001; 74(1–3):31–46. [PubMed: 11489481]

75■■. Dang W, Colvin OM, Brem H, Saltzman WM. Covalent coupling of methotrexate to dextran enhances the penetration of cytotoxicity into a tissue-like matrix. Cancer Res. 1994; 54(7):1729–1735. Authors demonstrated a novel technique to increase intratumoral drug penetration by attaching chemotherapeutic agents to dextran molecules. [PubMed: 7511049]

76. Weinberg BD, Patel RB, Wu H, et al. Model simulation and experimental validation of intratumoral chemotherapy using multiple polymer implants. Med Biol Eng Comput. 2008; 46(10):1039–1049. [PubMed: 18523817]

77. Oldendorf WH. Lipid solubility and drug penetration of the blood brain barrier. Proc Soc Exp Biol Med. 1974; 147(3):813–815. [PubMed: 4445171]

78. Kroll RA, Neuwelt EA. Outwitting the blood-brain barrier for therapeutic purposes. Osmotic opening and other means. Neurosurgery. 1998; 42(5):1083–1099. discussion 1099–1100. [PubMed: 9588554]

79. Rapoport SI. Advances in osmotic opening of the blood-brain barrier to enhance CNS chemotherapy. Expert Opin Investig Drugs. 2001; 10(10):1809–1818.

80. Sheikov N, Mcdannold N, Sharma S, Hynynen K. Effect of focused ultrasound applied with an ultrasound contrast agent on the tight junctional integrity of the brain microvascular endothelium. Ultrasound Med Biol. 2008; 34(7):1093–1104. [PubMed: 18378064]

81. Yang FY, Liu SH, Ho FM, Chang CH. Effect of ultrasound contrast agent dose on the duration of focused-ultrasound-induced blood–brain barrier disruption. J Acoust Soc Am. 2009; 126(6):3344–3349. [PubMed: 20000948]

82. Doolittle ND, Jahnke K, Belanger R, et al. Potential of chemo-immunotherapy and radioimmunotherapy in relapsed primary central nervous system (CNS) lymphoma. Leuk Lymphoma. 2007; 48(9):1712–1720. [PubMed: 17786706]

83. Fiandaca MS, Forsayeth JR, Dickinson PJ, Bankiewicz KS. Image-guided convection-enhanced delivery platform in the treatment of neurological diseases. Neurotherapeutics. 2008; 5(1):123–127. [PubMed: 18164491]

84. Bakhshi S, North RB. Implantable pumps for drug delivery to the brain. J Neurooncol. 1995; 26(2): 133–139. [PubMed: 8787855]

85. Hall WA, Sherr GT. Convection-enhanced delivery of targeted toxins for malignant glioma. Expert Opin Drug Deliv. 2006; 3(3):371–377. [PubMed: 16640497]

86. Broaddus WC, Gillies GT, Kucharczyk J. Minimally invasive procedures. Advances in image-guided delivery of drug and cell therapies into the central nervous system. Neuroimaging Clin N Am. 2001; 11(4):727–735. [PubMed: 11995427]

87. Rousseau J, Boudou C, Esteve F, Elleaume H. Convection-enhanced delivery of an iodine tracer into rat brain for synchrotron stereotactic radiotherapy. Int J Radiat Oncol Biol Phys. 2007; 68(3): 943–951. [PubMed: 17544004]

88. Astary GW, Kantorovich S, Carney PR, Mareci TH, Sarntinoranont M. Regional convection-enhanced delivery of gadolinium-labeled albumin in the rat hippocampus *in vivo*. J Neurosci Methods. 2010; 187(1):129–137. [PubMed: 20067808]

89. Ding D, Kanaly CW, Bigner DD, et al. Convection-enhanced delivery of free gadolinium with the recombinant immunotoxin MR1–1. J Neurooncol. 2010; 98(1):1–7. [PubMed: 19898744]

90. Sampson JH, Akabani G, Friedman AH, et al. Comparison of intratumoral bolus injection and convection-enhanced delivery of radiolabeled antitenascin monoclonal antibodies. Neurosurg Focus. 2006; 20(4):E14. [PubMed: 16709019]

91. Raghavan R, Brady Ml, Rodriguez-Ponce MI, Hartlep A, Pedain C, Sampson JH. Convection-enhanced delivery of therapeutics for brain disease and its optimization. Neurosurg Focus. 2006; 20(4):E12. [PubMed: 16709017]

92■■. Yin D, Valles FE, Fiandaca MS, et al. Optimal region of the putamen for image-guided convection-enhanced delivery of therapeutics in human and nonhuman primates. Neuroimage. 2010 (Epub ahead of print) Authors developed a technique to evaluate the optimal placement of a cannula for convection-enhanced delivery that limits the drug reflux and loss into the white matter tracts of the corpus callosum, which could be used to determine the 3D coordinates for surgical preplanning.

93. Kunwar S, Prados MD, Chang SM, et al. Direct intracerebral delivery of cintredekin besudotox (il13-pe38qqr) in recurrent malignant glioma. A report by the cintredekin besudotox intraparenchymal study group. J Clin Oncol. 2007; 25(7):837–844. [PubMed: 17327604]

94. Lonser RR, Warren KE, Butman Ja, et al. Real-time image-guided direct convective perfusion of intrinsic brainstem lesions. Technical note. J Neurosurg. 2007; 107(1):190–197. [PubMed: 17639894]

95. Murad GJ, Walbridge S, Morrison PF, et al. Real-time, image-guided, convection-enhanced delivery of interleukin 13 bound to pseudomonas exotoxin. Clin Cancer Res. 2006; 12(10):3145–3151. [PubMed: 16707614]

96. Croteau D, Walbridge S, Morrison PF, et al. Real-time *in vivo* imaging of the convective distribution of a low-molecular-weight tracer. J Neurosurg. 2005; 102(1):90–97. [PubMed: 15658101]

97. Lonser RR, Schiffman R, Robison RA, et al. Image-guided, direct convective delivery of glucocerebrosidase for neuronopathic gaucher disease. Neurology. 2007; 68(4):254–261. [PubMed: 17065591]

98. Cerullo N, Bufalino D, Daquino G. Progress in the use of gadolinium for NCT. Appl Radiat Isot. 2009; 67(7–8 Suppl):S157–160. [PubMed: 19410468]

99■■. De Stasio G, Rajesh D, Casalbore P, et al. Are gadolinium contrast agents suitable for gadolinium neutron capture therapy? Neurol Res. 2005; 27(4):387–398. Authors demonstrated techniques to determine the location of gadolinium (Gd) within a cell, to elucidate the rate of Gd uptake into the nucleus for optimal neutron capture therapy. [PubMed: 15949236]

100. Fujimoto T, Ichikawa H, Akisue T, et al. Accumulation of MRI contrast agents in malignant fibrous histiocytoma for gadolinium neutron capture therapy. Appl Radiat Isot. 2009; 67(7–8 Suppl):S355–358. [PubMed: 19386506]

101. Le UM, Shaker Ds, Sloat BR, Cui Z. A thermo-sensitive polymeric gel containing a gadolinium (Gd) compound encapsulated into liposomes significantly extended the retention of the Gd in tumors. Drug Dev Ind Pharm. 2008; 34(4):413–418. [PubMed: 18401783]

102. Mitin VN, Kulakov VN, Khokhlov VF, et al. Comparison of BNCT and GDNCT efficacy in treatment of canine cancer. Appl Radiat Isot. 2009; 67(7–8 Suppl):S299–301. [PubMed: 19428264]

103. Yang W, Barth RF, Wu G, et al. Convection enhanced delivery of boronated EGF as a molecular targeting agent for neutron capture therapy of brain tumors. J Neuroonco. 2009; 95(3):355–365.

104■■. Varenika V, Dickinson P, Bringas J, et al. Detection of infusate leakage in the brain using real-time imaging of convection-enhanced delivery. J Neurosurg. 2008; 109(5):874–880. Authors demonstrated the effect that reflux has on the distribution volume of convection-enhanced delivery and that without real-time imaging, reflux can lead to nontargeted delivery of drug into the cerebral spinal fluid and deep tissue regions of the brain. [PubMed: 18976077]

105. Yin D, Forsayeth J, Bankiewicz KS. Optimized cannula design and placement for convection-enhanced delivery in rat striatum. J Neurosci Methods. 2010; 187(1):46–51. [PubMed: 20026357]

106. Valles F, Fiandaca MS, Bringas J, et al. Anatomic compression caused by high-volume convection-enhanced delivery to the brain. Neurosurgery. 2009; 65(3):579–585. discussion 585–576. [PubMed: 19687704]

107. Gimenez F, Krauze MT, Valles F, et al. Image-guided convection-enhanced delivery of GDNF protein into monkey putamen. Neuroimage. 2010 (Epub ahead of print).

108. Sampson JH, Archer G, Pedain C, et al. Poor drug distribution as a possible explanation for the results of the precise trial. J Neurosurg. 2010 (Epub ahead of print).

109. Sandhu G, Solorio L, Broome A, et al. Whole animal imaging. Wiley Interdisciplinary Reviews: Systems Biology and Medicine Early View. 2010; 2:398–421.

110. Guthi JS, Yang SG, Huang G, et al. MRI-visible micellar nanomedicine for targeted drug delivery to lung cancer cells. Mol Pharm. 2009; 7(1):32–40.

111. Lammers T, Subr V, Peschke P, et al. Image-guided and passively tumour-targeted polymeric nanomedicines for radiochemotherapy. Br J Cancer. 2008; 99(6):900–910. [PubMed: 19238631]

112. Chen CS, Jounaidi Y, Su T, Waxman DJ. Enhancement of intratumoral cyclophosphamide pharmacokinetics and antitumor activity in a p450 2b11-based cancer gene therapy model. Cancer Gene Ther. 2007; 14(12):935–944. [PubMed: 17853921]

113. Li HL, Li S, Shao JY, et al. Pharmacokinetic and pharmacodynamic study of intratumoral injection of an adenovirus encoding endostatin in patients with advanced tumors. Gene Ther. 2008; 15(4):247–256. [PubMed: 18097470]

114. Xie M, Zhou L, Hu T, Yao M. Intratumoral delivery of paclitaxel-loaded poly(lactic-co-glycolic acid) microspheres for hep-2 laryngeal squamous cell carcinoma xenografts. Anticancer Drugs. 2007; 18(4):459–466. [PubMed: 17351398]

115. Luo TY, Shih YH, Chen CY, et al. Evaluating the potential of (188)re-ecd/lipiodol as a therapeutic radiopharmaceutical by intratumoral injection for hepatoma treatment. Cancer Biother Radiopharm. 2009; 24(5):535–541. [PubMed: 19877883]

116. Dunfee BL, Riaz A, Lewandowski RJ, et al. Yttrium-90 radioembolization for liver malignancies: prognostic factors associated with survival. J Vasc Interv Radiol. 2010; 21(1):90–95. [PubMed: 19939705]

117. Gulec SA, Fong Y. Yttrium 90 microsphere selective internal radiation treatment of hepatic colorectal metastases. Arch Surg. 2007; 142(7):675–682. [PubMed: 17638807]

118. Riaz A, Salem R. Yttrium-90 radioembolization in the management of liver tumors: Expanding the global experience. Eur J Nucl Med Mol Imaging. 2010; 37(3):451–452. [PubMed: 20033683]

119. Grahn AY, Bankiewicz KS, Dugich-Djordjevic M, et al. Nonpegylated liposomes for convection-enhanced delivery of topotecan and gadodiamide in malignant glioma: initial experience. J Neurooncol. 2009; 95(2):185–197. [PubMed: 19466380]

120. Vinchon-Petit S, Jarnet D, Paillard A, Benoit JP, Garcion E, Menei P. *In vivo* evaluation of intracellular drug-nanocarriers infused into intracranial tumours by convection-enhanced delivery: distribution and radiosensitisation efficacy. J Neurooncol. 2010; 97(2):195–205. [PubMed: 19768659]

121. Mackay JA, Deen DF, Szoka FC Jr. Distribution in brain of liposomes after convection enhanced delivery; modulation by particle charge, particle diameter and presence of steric coating. Brain Res. 2005; 1035(2):139–153. [PubMed: 15722054]

Executive summary

- Image guidance has the potential to transform the field of therapeutic delivery by providing minimally or noninvasive means to monitor or direct agent administration, activity and efficacy.
- Noninvasive characterization of drug distribution and treatment efficacy provides valuable insight to clinicians and researchers that can be used as feedback during intervention and can then be used to adjust treatment plans.
- Advances in computed tomography (CT), such as development of C-arm CT, combines the soft-tissue imaging capabilities of CT with the vascular imaging of digital subtraction angiography into a single imaging unit.
- Real-time imaging of convection-enhanced delivery will allow for optimized catheter placement and facilitate the adjustment of infusion parameters to limit reflux and maximize drug distribution.
- Implant precipitation of *in situ*-forming implant systems can be monitored *in vivo* and the rate of precipitation can be linearly correlated to the drug release.
- Particle-based systems provide a unique way to increase local concentrations of drug and radiopharmaceutics, while concurrently prolonging the exposure without inducing systemic toxicity.

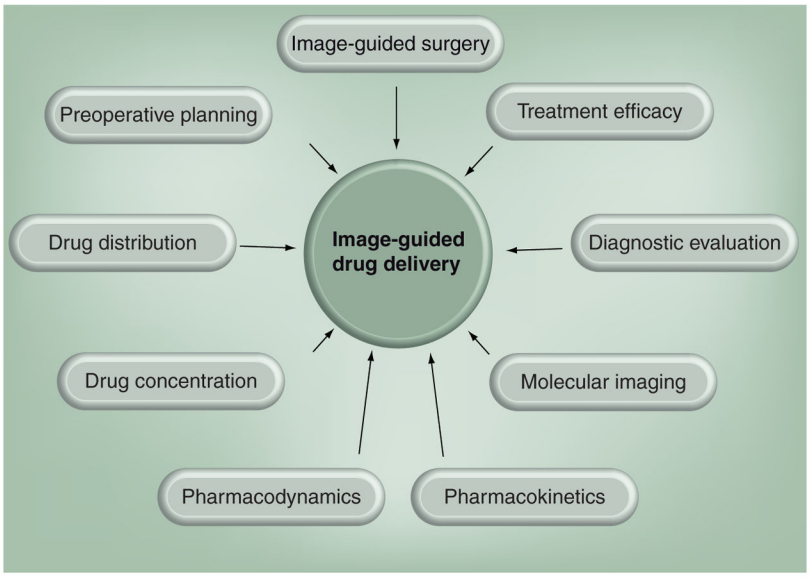

Figure 1.
Various components that comprise the field of image-guided drug delivery.

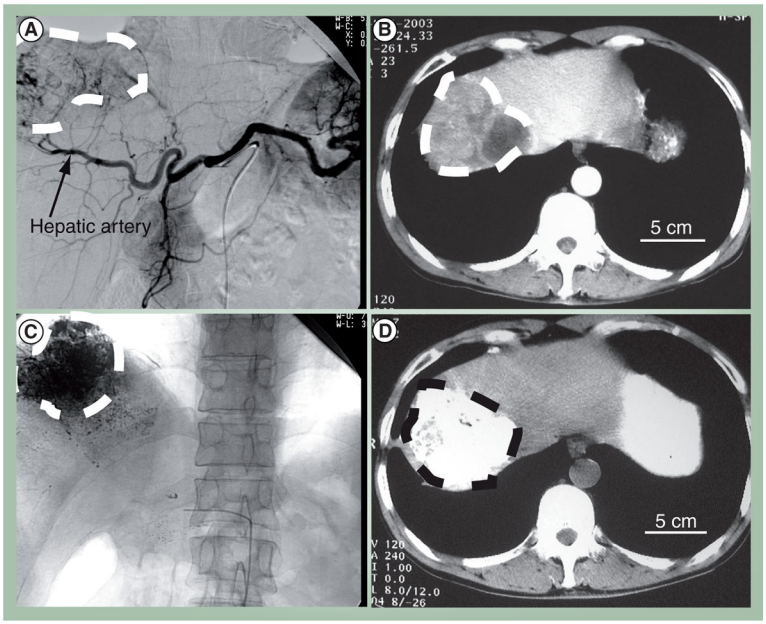

Figure 2. Pre- and peri-operative imaging for transarterial chemoembolization

(A) Digital subtraction angiography image of the celiac trunk shows a hepatocellular carcinoma tumor and its **(B)** corresponding feeding vessel branches of the hepatic artery. Contrast enhanced computed tomography (CT) shows a hypodense tumor region in the right liver lobe. **(C)** After transarterial chemoembolization treatment, iodized lipiodol is shown to accumulate in the tumor mass with planar x-ray imaging and **(D)** in noncontrast CT. All tumor regions are encircled by the dashed line.

Images reproduced with permission from Huimin Liang, Huazhong University of Science and Technology, China.

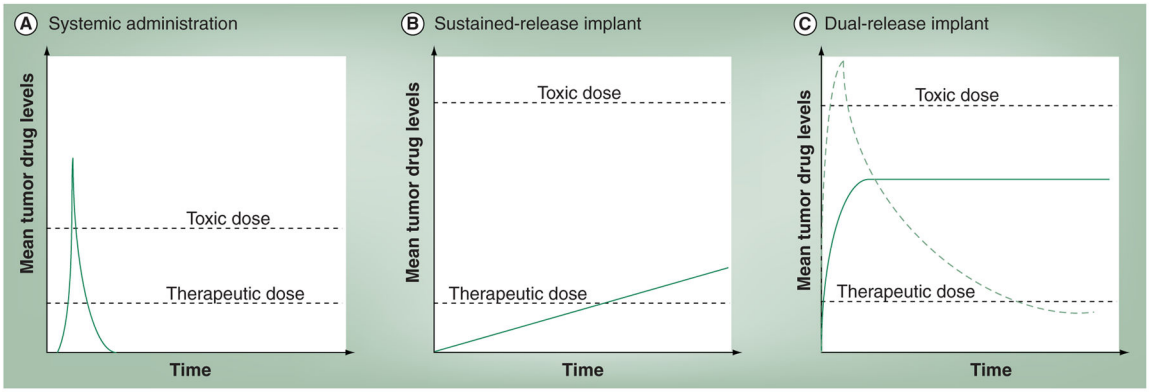

Figure 3. Idealized output of drug release systems

(A) Systemic bolus of intravenous chemotherapy results in a quick spike of the tumor drug concentration followed by short duration of therapeutic drug concentrations in the tumor. The therapeutic index is much narrower between **(A)** systemic chemotherapy and **(B & C)** local therapy. **(B)** Local implants with slow sustained drug release can maintain a therapeutic drug dose, however the long ramp up time to reach therapeutic doses may increase drug resistance. **(C)** Ideally, an implant has quick-burst drug release to quickly reach therapeutic drug levels followed by sustained delivery of drug to maintain therapeutic dosage (solid line). Implants that burst release too much of their loading drug dose will be unable to maintain tumor drug levels at a therapeutic dosage (dashed line).

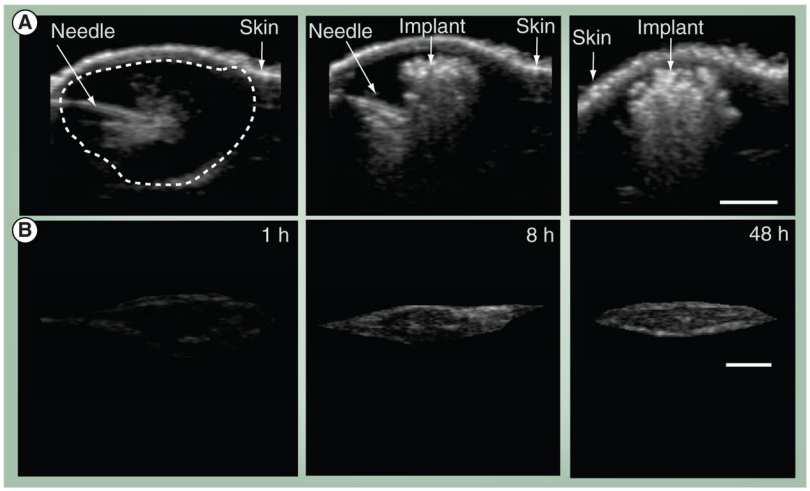

Figure 4. *In vivo* ultrasound imaging for the evaluation of implant formation

(A) Ultrasound images of an intratumoral injection of a 64-kDa *in situ* forming polymer solution, immediately before the polymer is injected, immediately after the polymer is injected and 24 h after the implant is injected and **(B)** isolated gray scale images of the *in vivo* subcutaneous 30-kDa implants over time at: 1, 8 and 48 h after implantation. The arrows indicate the location of the needle within the tumor volume as well as identifies the skin, the dashed line surrounds the tumor volume.

The scale bar represents 0.25 cm.

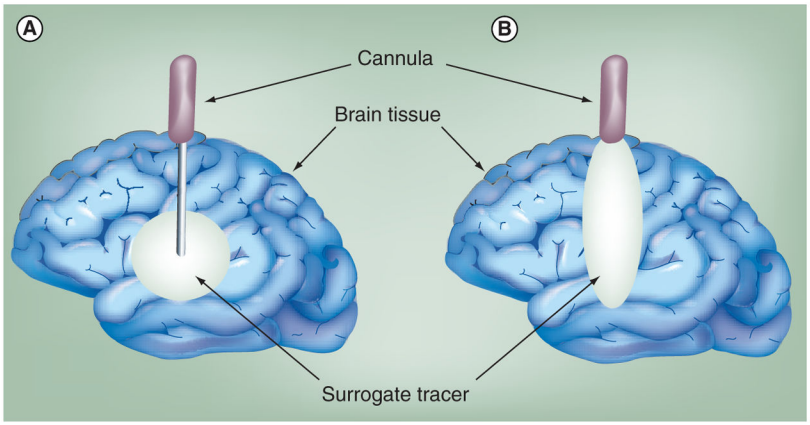

Figure 5. Convection-enhanced delivery

(A) An ideal delivery volume and **(B)** if reflux has occurred.

Table 1

Comparison of image-guided delivery techniques.

Delivery technique	Target	Systemic toxicity	Tumor penetration
Transarterial chemoembolization	Nonresectable hepatocellular carcinoma, cholangeal carcinoma and liver metastases	Leakage or blockage of nontumor vessels, portal thrombosis [29]	Generally good penetration, but depends on vessel blockage and presence of collateral circulation
Polymer Implants	Solid tumors	Local toxicity due to poor implant placement, low chance of systemic toxicity	Diffusion limitation (mm^3) [65,67]
Convection enhanced delivery	Malignant gliomas [75]	Leakage into white matter tracts [80], corpus callosum [80,94], sulci [93], ventricles [93]	Limited if refraction occurs (cm^3 in humans and nonhuman primates) [93]
Particles	Solid tumors and metastases [7,101]	Dependent on delivery technique [6,11,95,98,102]	Dependent on administration technique (mm^3–cm^3) [93,99,103]